THE JOURNAL OF PHYSICAL CHEMISTRY B

pubs.acs.org/JPCB Article

Ultrafast Vibrational Energy Transfer between Protein and Cofactor in a Flavoenzyme

Samantha J. O. Hardman,*[,§] Andreea I. Iorgu,[§] Derren J. Heyes, Nigel S. Scrutton, Igor V. Sazanovich, and Sam Hay*

Cite This: *J. Phys. Chem. B* 2020, 124, 5163−5168

Read Online

ACCESS | Metrics & More | Article Recommendations | Supporting Information

ABSTRACT: Protein motions and enzyme catalysis are often linked. It is hypothesized that ultrafast vibrations (femtosecond−picosecond) enhance the rate of hydride transfer catalyzed by members of the old yellow enzyme (OYE) family of ene-reductases. Here, we use time-resolved infrared (TRIR) spectroscopy in combination with stable "heavy" isotopic labeling (^{2}H, ^{13}C, ^{15}N) of protein and/or cofactor to probe the vibrational energy transfer (VET) between pentaerythritol tetranitrate reductase (a member of the OYE family) and its noncovalently bound flavin mononucleotide (FMN) cofactor. We show that when the FMN cofactor is photoexcited with visible light, vibrational energy is transferred from the flavin to the surrounding protein environment on the picosecond timescale. This finding expands the scope of VET investigation in proteins, which are limited by suitable intrinsic probes, and may have implications in the understanding of the mechanism of recently discovered photoactive flavoenzymes.

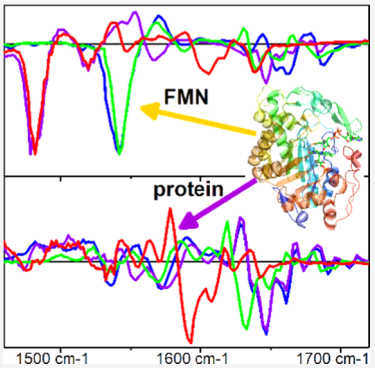

How protein motions influence enzyme catalysis is a contemporary issue in enzymology. Protein dynamics occur over a broad range of temporal (femtoseconds−seconds) and spatial (0.1−100 Å) scales and can be probed using a variety of structural, spectroscopic, and computational approaches. The role of "slow" long-range protein conformational changes, typically taking place on micro- to millisecond timescales, in substrate binding and allosteric regulation is well documented in the literature.[1,2] However, the role of "fast" femto- to nanosecond protein motions in enzymatic catalysis is more contentious.[3−5] It is hypothesized that fast bond vibrations support hydride transfer from the nicotinamide (NAD(P)H) coenzyme to the flavin mononucleotide (FMN, Figure 1A) cofactor in the old yellow enzyme (OYE) family of ene-reductases.[6] The reductive hydride transfer step, and the role of motions in catalysis, has been extensively studied in a range of OYE homologues, which have been used as model systems to study enzymatic H-transfer,[7−10] but direct experimental evidence that supports the role of protein vibrations in H-transfer in these enzymes is currently lacking.

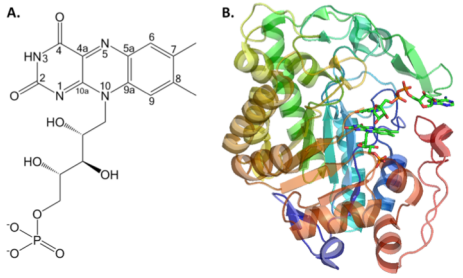

Figure 1. (A) FMN; (B) X-ray crystal structure of the PETNR:FMN·$NADH_4$ complex (PDB: 3KFT) showing $NADH_4$ and FMN in green.[7]

It has previously been shown that incorporation of different stable "heavy" isotopes (^{2}H, ^{13}C, ^{15}N) in both the protein scaffold and/or the FMN cofactor of the OYE pentaerythritol tetranitrate reductase (PETNR) influences the kinetics of reductive hydride transfer.[11] A potentially powerful technique to further probe the role of fast protein vibrations during this reaction is time-resolved infrared (TRIR) spectroscopy, which has been widely used to follow the photoreactions of numerous flavin-containing blue-light-utilizing (BLUF) and light, oxygen, or voltage sensing (LOV) photoreceptors.[12−14] Specific isotope substitution subtly changes the frequency of bond vibrations, allowing assignment of spectral changes in the mid-infrared (IR) region. Changes in bond frequencies may also perturb any vibrational energy transfer (VET) within the system, and isotope labeling may affect the electrostatics.[15] Herein, we have used TRIR to further investigate a hypothesized vibronic coupling between the FMN and the protein scaffold in PETNR.[11] TRIR measurements, collected after photoexcitation of the FMN at 450 nm, were performed

Received: June 1, 2020
Published: June 4, 2020

https://dx.doi.org/10.1021/acs.jpcb.0c04929
J. Phys. Chem. B 2020, 124, 5163−5168

on four isotopologues of PETNR (Figure 1B): ^{15}N-PETNR:^{15}N-FMN; ^{15}N-PETNR:^{2}H^{13}C^{15}N-FMN; ^{2}H^{15}N-PETNR:^{2}H^{15}N-FMN; and ^{2}H^{13}C^{15}N-PETNR: ^{2}H^{13}C^{15}N-FMN. All samples contained the ^{15}N isotope (which allows sample quality control by NMR), so the notation has been abbreviated as: PETNR:FMN, PETNR:^{2}H^{13}C-FMN, ^{2}H-PETNR:^{2}H-FMN, and ^{2}H^{13}C-PETNR: ^{2}H^{13}C-FMN, respectively. All measurements were performed in D_2O, so the majority of solvent-exchangeable protons will be ^{2}H and the sample specified as ^{2}H labeled also includes labeling of nonexchangeable hydrogens.[16] TRIR data are shown in Figure 2 (static IR spectra are shown in Figure S1, and the TRIR data

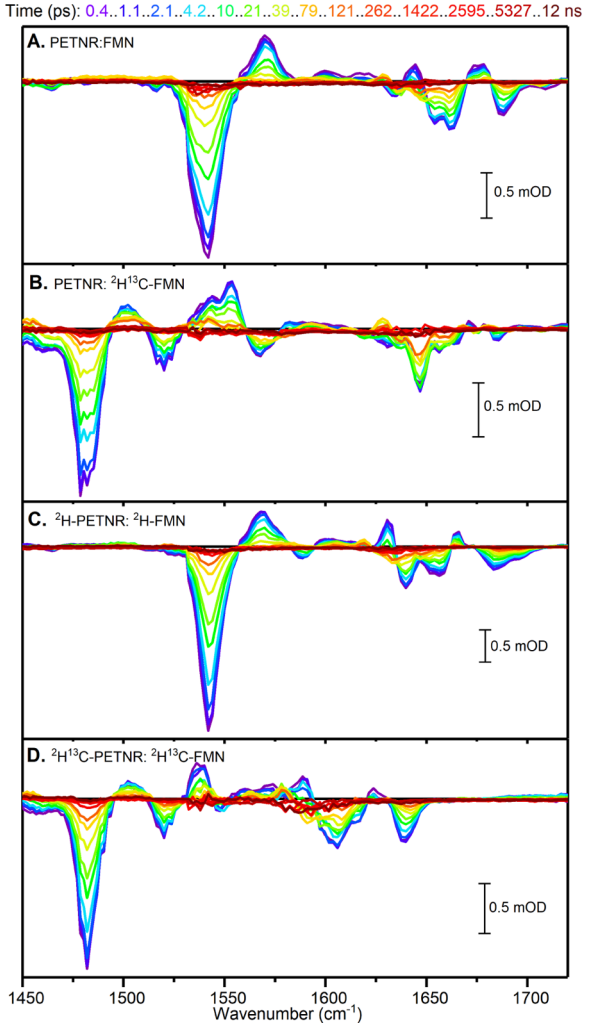

Figure 2. TRIR spectra of PETNR:FMN isotopologues, recorded at selected times after photoexcitation at 450 nm. (A) PETNR:FMN; (B) PETNR:^{2}H^{13}C-FMN; (C) ^{2}H-PETNR:^{2}H-FMN; and (D) ^{2}H^{13}C-PETNR:^{2}H^{13}C-FMN.

are shown in more detail in Figures S2–S6). Negative spectral features represent absorption features (bond vibrations) that have been depopulated after photoexcitation, while positive spectral features represent newly populated states, bond vibrations of either electronically excited states or reaction intermediates.

To study the structural changes that occur after photoexcitation, the TRIR data were globally analyzed using a sequentially evolving model of four components. Three lifetime components were variable, and one that represents any long-lived (>12 ns) species was fixed. The fitted lifetimes are shown in Table S1. The evolution associated difference spectra (EADS), which represent the spectral evolution over time are shown normalized to the most intense feature in Figure 3 (and as relative intensities for each sample in Figure

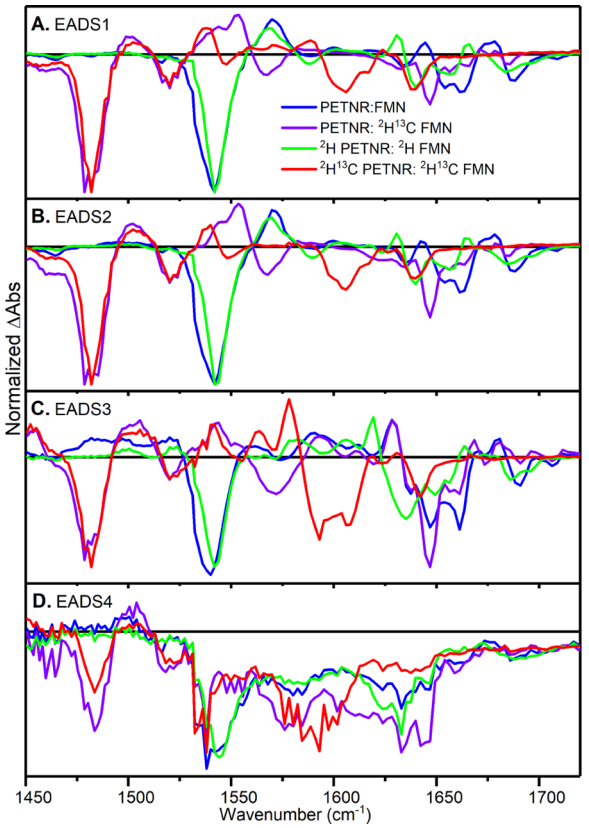

Figure 3. EADS, normalized to the most intense negative feature, resulting from a global analysis of TRIR data using a sequential model of four interconverting components. Data is plotted as relative intensities of each sample in Figure S7. EADS1 (A) converts to EADS2 (B) with τ_1, which converts to EADS3 (C) with τ_2, which converts to EADS4 (D) with τ_3. EADS4 then persists for the duration of the data collection window (12 ns).

S7). The final, nondecaying, component, EADS4 (formed with a lifetime of ~100 ps) has a very low intensity (2–3% of initial signal), and no positive features, and is most likely to arise from sample degradation.

EADS1 and EADS2 for each isotopologue are virtually identical in shape, but differ in intensity (Figure S7), meaning that the first transition ($\tau_1 \approx 4.4$ ps) does not result in any structural change and thus can be assigned to FMN excited state relaxation. The TRIR features for unlabeled FMN and FAD in the solution have been very well characterized[17,18] and correlate well with the major spectral features observed here (Figure 3A,B). The major negative feature observed at ~1542 cm^{-1} is assigned to the C10a = N1 stretch, and the smaller feature at ~1588 cm^{-1} is assigned to the C4a = N5 stretch. The carbonyl groups on the flavin also have distinct features at ~1660 (C2=O) and 1709 cm^{-1} (C4=O). Between these two major sets of features are a number of low-intensity peaks, which are assigned to the C=C and C–N bonds in the isoalloxazine moiety (FMN rings). In a previous study of isotopically labeled FAD in an unlabeled flavoprotein, it was

https://dx.doi.org/10.1021/acs.jpcb.0c04929
J. Phys. Chem. B 2020, 124, 5163–5168

found that ^{15}N substitutions shift the C═N peaks to slightly lower wavenumbers (by ∼10 cm^{-1}), but do not significantly affect the C═O modes. ^{13}C substitutions in contrast shift both the C═N and C═O vibrational modes more substantially (up to 45 cm^{-1}).[13] A study of unlabeled FAD in isotopically labeled flavoprotein observed that the C═O modes of the flavin appear to be largely insensitive to ^{13}C-labeling of the protein.[19] In agreement with those previous studies, when comparing varying FMN isotopologues within the same protein environment, it does not appear that ^{15}N labeling alone has any significant effect on the spectra (see the Supporting Information for PETNR: unlabeled-FMN data), whereas $^{2}H^{13}C^{15}N$ labeling does shift the major C═N feature by 60 cm^{-1} to lower frequencies. When comparing the same FMN isotopologue with varying protein isotopologues, it is clear that while the C═N features are unaffected, the modes assigned to the C═C and C−N ring features and the C═O bonds are shifted to lower wavenumbers in "heavier" protein environments. The effect is also visible in the ^{2}H labeled sample.

In all data sets, EADS3 contains significantly different features to those in EADS1 and EADS2, indicating a significant structural change associated with the ∼20 ps transition from EADS2 to EADS3. These changes may be in either the FMN or the protein. Only the FMN absorbs in the visible spectral region, so we can be confident that any changes observed in the visible spectrum after photoexcitation correspond to changes in the FMN. Time-resolved visible spectroscopy, collected over 3 ns on a PETNR: unlabeled-FMN sample, globally analyzed with three variable components gave fitted lifetimes of 5.0, 18.9, and 86.3 ps (Figure S8). These values correlate well with those of changes in the IR region (4.6, 19.6, and 92.3 ps for the same isotopologue), implying that in both cases it is the changes in the FMN that dominate the spectra. Because of the simple sequential model used for the global analysis of the TRIR data and the spectral dominance of the FMN features, it is likely that there will be some contributions from the excited state of FMN throughout. Thus, to extract the signature of the structural change that occurs between EADS2 and EADS3, each EADS3 (potentially a mixture of protein and FMN signals) had the corresponding EADS1 (primarily FMN signal) subtracted after normalization to the intensity of the major FMN bleach feature to yield the spectra shown in Figure 4.

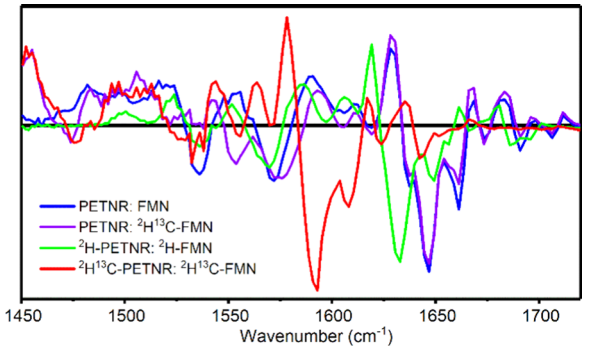

Figure 4. EADS3−EADS1 (both normalized to major FMN bleach) difference spectra for PETNR: FMN (blue), PETNR:$^{2}H^{13}C$-FMN (violet), ^{2}H-PETNR:^{2}H-FMN (green), and $^{2}H^{13}C$-PETNR:$^{2}H^{13}C$-FMN (red).

The obvious similarities in the profile shown in Figure 4 above 1550 cm^{-1} between the same protein isotopologues with different cofactors clearly imply that these features originate from the protein itself. ^{2}H and ^{13}C-labeling of the protein causes major spectral features to shift to lower frequencies by ∼14 and ∼42 cm^{-1}, respectively. Similar shifts have been observed after the ^{13}C-labeling of a BLUF domain protein.[20] There are 11 amino acid residues located <4 Å from the main isoalloxazine ring of the FMN (Figure S9). The IR absorption spectra of these residues overlap to such a large extent[21,22] that even without considering the effects of the local environment (surrounding amino acids, solvent, etc.), it is virtually impossible to deconvolute them. More generally, protein amide I bands (ca. 1600−1700 cm^{-1}, primarily assigned to C═O vibrations with some contributions from the C−N stretch and N−H deformation) have been shown to shift 42−45 cm^{-1} with ^{13}C-labeling, but only a few wavenumbers with ^{15}N and/or ^{2}H labeling,[23−25] which correlates well the observations recorded here. In the EADS3 spectra, in addition to the bleach features assigned to the protein, there are positive features not present in EADS1/2. For all of the samples, the most intense FMN bleach (∼1540 cm^{-1} for all but $^{2}H^{13}C$-FMN at ∼1482 cm^{-1}) has a positive transient band on the lower energy side (at ca. 1502 and 1454 cm,$^{-1}$ respectively). Such a pattern is typical for the "hot" (vibrationally excited) electronic ground-state signal, where the bleach of the "cold" ground state is accompanied by transient bands corresponding to the vibrationally hot ground state, appearing just slightly shifted to lower energy due to vibrational anharmonicity.[26] Similar low-energy positive features are also observed for the protein bleaches: the most intense PETNR bleach (at 1647 cm^{-1} for PETNR, 1633 cm^{-1} for ^{2}H-PETNR, and 1593 cm^{-1} for $^{2}H^{13}C$-PETNR) is accompanied with the positive transient band on the low-energy side (at 1628, 1619, and 1578 cm,$^{-1}$ respectively), which we assign to vibrationally excited protein. One can clearly see that on the two-dimensional (2D) plots of TRIR data (at ca. 1628 cm^{-1} in Figures S2−S4, at ca. 1619 cm^{-1} in Figure S5, and at ca. 1578 cm^{-1} in Figure S6), the positive transient signal, which was not there at time zero, gradually appears at around 10 ps, and then gradually decays after 100 ps. This strongly indicates that there is VET from the FMN cofactor to the PETNR protein during the transition from EADS2 to EADS3.

To refine the kinetic fit parameters, single wavenumber kinetic traces were selected for each sample at significant features originating from, primarily, the FMN and the protein (Figure S7 and Table S2). These traces were fitted with a triple exponential function using shared lifetime parameters for each sample (Figures S10 and S11). A common trend across all data sets (data for PETNR:FMN is shown in Figure 5) is that for features that primarily derive from FMN a large initial signal relaxes with the three lifetime components. In contrast, the features with a more significant contribution from the PETNR do not have large amplitudes for the fastest kinetic component. However, the second and third lifetimes correspond to a growth and recovery of the protein signals and suggest that there are vibrational excitation and subsequent relaxation on these timescales. This is in agreement with the results of the global analysis, indicating that after electronic excitation of the FMN, vibrational energy is transferred to the protein on a ∼25 ps timescale. This lifetime is very similar to that of the electronic relaxation of the FMN (∼20 ps as derived from the TR-vis measurements), which initiates the VET to the protein.

https://dx.doi.org/10.1021/acs.jpcb.0c04929
J. Phys. Chem. B 2020, 124, 5163−5168

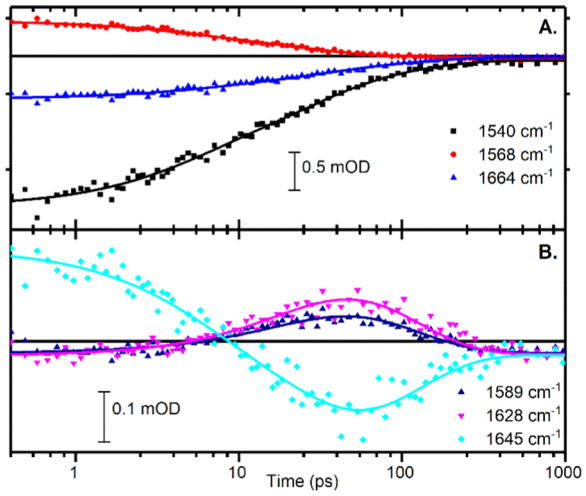

Figure 5. Kinetic traces (points) with lines showing fit to multiexponential function for the PETNR:FMN data set; fitted shared lifetimes are τ_1 = 3.4 ± 0.4, τ_2 = 25.1 ± 3.4, and τ_3 = 97.0 ± 11.9 ps. (A) Kinetics originating primarily from FMN and (B) kinetics originating primarily from protein.

Therefore, it is difficult to obtain the "pure" rate of VET as such, and the rate we observe is the convolution of the two.

The kinetic fitting also reveals noticeable differences in lifetimes between protein and FMN isotopologues, resulting in the calculated kinetic isotope effects (KIEs) shown in Table 1. While the uncertainty in the kinetic fit parameters means that many of the apparent KIEs may not be significant, there are some noticeable trends. The KIEs appear to largely arise from ^{13}C rather than ^{2}H, which suggests that the KIEs may arise from a perturbation in mid-IR bond frequencies (much larger for ^{13}C than ^{2}H). The largest KIEs are on the first lifetime, τ_1 (the major FMN excited state relaxation component). The second two lifetime components, τ_2 and τ_3, which are assigned, at least partially, to transfer vibrational energy to the protein and subsequent relaxation, show smaller KIEs, and the only KIE that may be significant is the protein ^{13}C KIE on τ_2. We also observe an apparent increase in VET between the FMN and the protein as the mass of either species increases (Figure S12). Previous work has suggested that there is a mass-dependent vibronic coupling of protein and FMN motions to FMN electronically excited state(s), which manifests as KIEs on the nanosecond FMN fluorescence lifetime components.[11] The KIEs measured here help to rationalize this finding as fluorescence competes with nonradiative relaxation, which is expected to be dependent on the vibrational coupling of the FMN to protein and/or solvent.

Collectively, the data presented in this study provides direct evidence of VET between the FMN cofactor and the protein and can be interpreted as follows. After photoexcitation, the electronically excited states of FMN relax to vibrationally hot electronic ground states; the most significant lifetimes for this process are around 4.4 and 20 ps. Over half of the excited state signal is lost within 10−20 ps. From this vibrationally hot FMN, there is then VET to the surrounding protein environment, which we do not resolve as a separate kinetic component because such VET process is on a similar timescale to, and thus convoluted with, the second, dominant, FMN electronic decay. Vibrational cooling to the solvent often occurs on similar 10−20 ps timescales as we observe here.[27] Studies of VET in proteins with natural heme or unnatural azulene-based probes observed faster sub-10 ps processes; the rates of which were linked to the strength of H-bonding and van der Waals interactions rather than covalent linkages.[28,29] These studies are facilitated by the very short heme excited state lifetimes (typically 2−6 ps),[30] whereas here we have been unable to clearly resolve the VET rate in PETNR. However, it does appear that VET in PETNR occurs on slower timescales than in those other proteins, suggesting that the flavin behaves differently to these other cofactors and/or VET occurs over longer distances and/or through weaker H-bond and/or van der Walls interactions in PETNR. Although it is likely that the FMN is more strongly vibrationally coupled to the protein than the solvent, the energy transfer may occur directly and/or indirectly through the protein solvation shell. The final relaxation step, occurring over several hundred ps, follow the remaining vibrationally hot states (and a small amount of remaining electronically excited FMN) returning to ground-state equilibrium with energy dissipation through the protein, FMN, and/or solvent.

In conclusion, we suggest that photoexcitation of the FMN in PETNR leads to VET to the surrounding protein and solvent environment on a timescale of around 20 ps. While previous TRIR studies of flavin photoreceptors have detected changes in the protein structure, the signaling response, on μs timescales,[12,31] and in one case instantaneous perturbation of the binding site after photoexcitation,[19] this is, to our knowledge, the first observation of VET from the flavin to the surrounding protein environment on ps timescales. This finding opens new avenues of investigation in studies of VET in proteins, which are typically hampered by a lack of suitable intrinsic probes. Further, examples of both natural and engineered/artificial photoactivated flavoenzymes have recently been documented.[32−34] It seems likely that visible photoexcitation of the flavin in these enzymes will also lead to VET to surrounding protein residues and water molecules in the active site. How this impacts (photo)catalysis remains to be seen, but the VET will lead to local heating, which has the potential to be catalytic.[35] Ultrafast TRIR experiments provide a means of probing such VET and have the potential to aid in future enzyme engineering efforts.

Table 1. Apparent KIEs Determined from the Data in Figure S11 of the Supporting Information

sample[a]	isotope effect	KIE(τ_1)	KIE(τ_2)	KIE(τ_3)
PETNR:FMN vs PETNR:$^{2}H^{13}C$-FMN	$^{2}H^{13}C$ KIE on FMN	1.26 ± 0.31	1.02 ± 0.22	1.05 ± 0.15
PETNR:FMN vs ^{2}H-PETNR:^{2}H-FMN	^{2}H KIE on PETNR + FMN	0.95 ± 0.18	1.05 ± 0.18	1.09 ± 0.16
PETNR:FMN vs $^{2}H^{13}C$-PETNR:$^{2}H^{13}C$-FMN	$^{2}H^{13}C$ KIE on PETNR + FMN	1.49 ± 0.41	1.19 ± 0.32	1.08 ± 0.20
PETNR:$^{2}H^{13}C$-FMN vs $^{2}H^{13}C$-PETNR:$^{2}H^{13}C$-FMN	$^{2}H^{13}C$-KIE on PETNR	1.19 ± 0.32	1.17 ± 0.31	1.02 ± 0.19

[a]All samples contain ^{15}N.

https://dx.doi.org/10.1021/acs.jpcb.0c04929
J. Phys. Chem. B 2020, 124, 5163−5168

■ ASSOCIATED CONTENT

Supporting Information

The Supporting Information is available free of charge at https://pubs.acs.org/doi/10.1021/acs.jpcb.0c04929.

Experimental methods, static IR spectra, time-resolved IR and visible data, kinetic fitting parameters and results (PDF)

■ AUTHOR INFORMATION

Corresponding Authors

Samantha J. O. Hardman − *Manchester Institute of Biotechnology and Department of Chemistry, Faculty of Science and Engineering, The University of Manchester, Manchester M1 7DN, United Kingdom*; Email: samantha.hardman@manchester.ac.uk

Sam Hay − *Manchester Institute of Biotechnology and Department of Chemistry, Faculty of Science and Engineering, The University of Manchester, Manchester M1 7DN, United Kingdom*; orcid.org/0000-0003-3274-0938; Email: sam.hay@manchester.ac.uk

Authors

Andreea I. Iorgu − *Manchester Institute of Biotechnology and Department of Chemistry, Faculty of Science and Engineering, The University of Manchester, Manchester M1 7DN, United Kingdom*; orcid.org/0000-0002-1363-3697

Derren J. Heyes − *Manchester Institute of Biotechnology and Department of Chemistry, Faculty of Science and Engineering, The University of Manchester, Manchester M1 7DN, United Kingdom*

Nigel S. Scrutton − *Manchester Institute of Biotechnology and Department of Chemistry, Faculty of Science and Engineering, The University of Manchester, Manchester M1 7DN, United Kingdom*; orcid.org/0000-0002-4182-3500

Igor V. Sazanovich − *Central Laser Facility, Research Complex at Harwell, Science and Technology Facilities Council, Didcot OX11 0QX, United Kingdom*

Complete contact information is available at: https://pubs.acs.org/10.1021/acs.jpcb.0c04929

Author Contributions

[§]S.J.O.H. and A.I.I. contributed equally to this work.

Notes

The authors declare no competing financial interest.

■ ACKNOWLEDGMENTS

A.I.I. was an early stage researcher supported by the EU's Seventh Framework Programme through the Marie Curie Initial Training Network MAGIC (Grant Agreement No. 606831). This work was also supported by the Biotechnology and Biological Sciences Research Council (BBSRC; BB/M007065/1 and BB/S003320/1). Time-resolved infrared measurements were performed through program access support of the UK Science and Technology Facilities Council (STFC). Time-resolved visible measurements were performed at the Ultrafast Biophysics Facility, Manchester Institute of Biotechnology, as funded by BBSRC Alert14 Award BB/M011658/1.

■ REFERENCES

(1) Pelton, J. T.; McLean, L. R. Spectroscopic Methods for Analysis of Protein Secondary Structure. *Anal. Biochem.* **2000**, *277*, 167−176.

(2) Levantino, M.; Yorke, B. A.; Monteiro, D. C. F.; Cammarata, M.; Pearson, A. R. Using synchrotrons and XFELs for time-resolved X-ray crystallography and solution scattering experiments on biomolecules. *Curr. Opin. Struct. Biol.* **2015**, *35*, 41−48.

(3) Hay, S.; Scrutton, N. S. Good vibrations in enzyme-catalysed reactions. *Nat. Chem.* **2012**, *4*, 161−168.

(4) Kohen, A. Role of Dynamics in Enzyme Catalysis: Substantial versus Semantic Controversies. *Acc. Chem. Res.* **2015**, *48*, 466−473.

(5) Pagano, P.; Guo, Q.; Ranasinghe, C.; Schroeder, E.; Robben, K.; Häse, F.; Ye, H.; Wickersham, K.; Aspuru-Guzik, A.; Major, D. T.; Gakhar, L.; Kohen, A.; Cheatum, C. M. Oscillatory Active-Site Motions Correlate with Kinetic Isotope Effects in Formate Dehydrogenase. *ACS Catal.* **2019**, *9*, 11199−11206.

(6) Toogood, H. S.; Gardiner, J. M.; Scrutton, N. S. Biocatalytic Reductions and Chemical Versatility of the Old Yellow Enzyme Family of Flavoprotein Oxidoreductases. *ChemCatChem* **2010**, *2*, 892−914.

(7) Pudney, C. R.; Hay, S.; Levy, C.; Pang, J. Y.; Sutcliffe, M. J.; Leys, D.; Scrutton, N. S. Evidence To Support the Hypothesis That Promoting Vibrations Enhance the Rate of an Enzyme Catalyzed H-Tunneling Reaction. *J. Am. Chem. Soc.* **2009**, *131*, 17072−17073.

(8) Pudney, C. R.; Guerriero, A.; Baxter, N. J.; Johannissen, L. O.; Waltho, J. P.; Hay, S.; Scrutton, N. S. Fast Protein Motions Are Coupled to Enzyme H-Transfer Reactions. *J. Am. Chem. Soc.* **2013**, *135*, 2512−2517.

(9) Iorgu, A. I.; Hedison, T. M.; Hay, S.; Scrutton, N. S. Selectivity through discriminatory induced fit enables switching of NAD(P)H coenzyme specificity in Old Yellow Enzyme ene-reductases. *FEBS J.* **2019**, *286*, 3117−3128.

(10) Hardman, S. J.; Pudney; C, R.; Hay, S.; Scrutton, N. S. Excited State Dynamics Can Be Used to Probe Donor-Acceptor Distances for H-Tunneling Reactions Catalyzed by Flavoproteins. *Biophys. J.* **2013**, *105*, 2549−2558.

(11) Longbotham, J. E.; Hardman, S. J. O.; Görlich, S.; Scrutton, N. S.; Hay, S. Untangling Heavy Protein and Cofactor Isotope Effects on Enzyme-Catalyzed Hydride Transfer. *J. Am. Chem. Soc.* **2016**, *138*, 13693−13699.

(12) Brust, R.; Lukacs, A.; Haigney, A.; Addison, K.; Gil, A.; Towrie, M.; Clark, I. P.; Greetham, G. M.; Tonge, P. J.; Meech, S. R. Proteins in Action: Femtosecond to Millisecond Structural Dynamics of a Photoactive Flavoprotein. *J. Am. Chem. Soc.* **2013**, *135*, 16168−16174.

(13) Haigney, A.; Lukacs, A.; Brust, R.; Zhao, R.-K.; Towrie, M.; Greetham, G. M.; Clark, I.; Illarionov, B.; Bacher, A.; Kim, R.-R.; Fischer, M.; Meech, S. R.; Tonge, P. J. Vibrational Assignment of the Ultrafast Infrared Spectrum of the Photoactivatable Flavoprotein AppA. *J. Phys. Chem. B* **2012**, *116*, 10722−10729.

(14) Iuliano, J. N.; Gil, A. A.; Laptenok, S. P.; Hall, C. R.; Tolentino Collado, J.; Lukacs, A.; Hag Ahmed, S. A.; Abyad, J.; Daryaee, T.; Greetham, G. M.; Sazanovich, I. V.; Illarionov, B.; Bacher, A.; Fischer, M.; Towrie, M.; French, J. B.; Meech, S. R.; Tonge, P. J. Variation in LOV Photoreceptor Activation Dynamics Probed by Time-Resolved Infrared Spectroscopy. *Biochemistry* **2018**, *57*, 620−630.

(15) Ranasinghe, C.; Pagano, P.; Sapienza, P. J.; Lee, A. L.; Kohen, A.; Cheatum, C. M. Isotopic Labeling of Formate Dehydrogenase Perturbs the Protein Dynamics. *J. Phys. Chem. B* **2019**, *123*, 10403−10409.

(16) Iorgu, A. I.; Cliff, M. J.; Waltho, J. P.; Scrutton, N. S.; Hay, S. Chapter Six - Isotopically labeled flavoenzymes and their uses in probing reaction mechanisms. In *Methods Enzymol*; Palfey, B. A., Ed.; Academic Press, 2019; Vol. *620*, pp 145−166.

(17) Kondo, M.; Nappa, J.; Ronayne, K. L.; Stelling, A. L.; Tonge, P. J.; Meech, S. R. Ultrafast Vibrational Spectroscopy of the Flavin Chromophore. *J. Phys. Chem. B* **2006**, *110*, 20107−20110.

(18) Haigney, A.; Lukacs, A.; Zhao, R.-K.; Stelling, A. L.; Brust, R.; Kim, R.-R.; Kondo, M.; Clark, I.; Towrie, M.; Greetham, G. M.; Illarionov, B.; Bacher, A.; Römisch-Margl, W.; Fischer, M.; Meech, S. R.; Tonge, P. J. Ultrafast Infrared Spectroscopy of an Isotope-Labeled Photoactivatable Flavoprotein. *Biochemistry* **2011**, *50*, 1321−1328.

(19) Lukacs, A.; Haigney, A.; Brust, R.; Zhao, R.-K.; Stelling, A. L.; Clark, I. P.; Towrie, M.; Greetham, G. M.; Meech, S. R.; Tonge, P. J. Photoexcitation of the Blue Light Using FAD Photoreceptor AppA Results in Ultrafast Changes to the Protein Matrix. *J. Am. Chem. Soc.* **2011**, *133*, 16893−16900.
(20) Lukacs, A.; Brust, R.; Haigney, A.; Laptenok, S. P.; Addison, K.; Gil, A.; Towrie, M.; Greetham, G. M.; Tonge, P. J.; Meech, S. R. BLUF Domain Function Does Not Require a Metastable Radical Intermediate State. *J. Am. Chem. Soc.* **2014**, *136*, 4605−4615.
(21) Wolpert, M.; Hellwig, P. Infrared spectra and molar absorption coefficients of the 20 alpha amino acids in aqueous solutions in the spectral range from 1800 to 500cm−1. *Spectrochim. Acta, Part A* **2006**, *64*, 987−1001.
(22) Barth, A. Infrared spectroscopy of proteins. *Biochim. Biophys. Acta, Bioenerg.* **2007**, *1767*, 1073−1101.
(23) Haris, P. I.; Robillard, G. T.; Van Dijk, A. A.; Chapman, D. Potential of carbon-13 and nitrogen-15 labeling for studying protein-protein interactions using Fourier-transform infrared spectroscopy. *Biochemistry* **1992**, *31*, 6279−6284.
(24) Baello, B. I.; Pancoska, P.; Keiderling, T. A. Enhanced Prediction Accuracy of Protein Secondary Structure Using Hydrogen Exchange Fourier Transform Infrared Spectroscopy. *Anal. Biochem.* **2000**, *280*, 46−57.
(25) Haris, P. I. Can infrared spectroscopy provide information on protein-protein interactions? *Biochem. Soc. Trans.* **2010**, *38*, 940−946.
(26) Doorley, G. W.; Wojdyla, M.; Watson, G. W.; Towrie, M.; Parker, A. W.; Kelly, J. M.; Quinn, S. J. Tracking D. N. A. Excited States by Picosecond-Time-Resolved Infrared Spectroscopy: Signature Band for a Charge-Transfer Excited State in Stacked Adenine−Thymine Systems. *J. Phys. Chem. Lett.* **2013**, *4*, 2739−2744.
(27) Qin, Y.; Jia, M.; Yang, J.; Wang, D.; Wang, L.; Xu, J.; Zhong, D. Molecular Origin of Ultrafast Water−Protein Coupled Interactions. *J. Phys. Chem. Lett.* **2016**, *7*, 4171−4177.
(28) Leitner, D. M.; Pandey, H. D.; Reid, K. M. Energy Transport across Interfaces in Biomolecular Systems. *J. Phys. Chem. B* **2019**, *123*, 9507−9524.
(29) Baumann, T.; Hauf, M.; Schildhauer, F.; Eberl, K. B.; Durkin, P. M.; Deniz, E.; Löffler, J. G.; Acevedo-Rocha, C. G.; Jaric, J.; Martins, B. M.; Dobbek, H.; Bredenbeck, J.; Budisa, N. Site-Resolved Observation of Vibrational Energy Transfer Using a Genetically Encoded Ultrafast Heater. *Angew. Chem., Int. Ed.* **2019**, *58*, 2899−2903.
(30) Li, P.; Sage, J. T.; Champion, P. M. Probing picosecond processes with nanosecond lasers: Electronic and vibrational relaxation dynamics of heme proteins. *J. Chem. Phys.* **1992**, *97*, 3214−3227.
(31) Gil, A. A.; Laptenok, S. P.; French, J. B.; Iuliano, J. N.; Lukacs, A.; Hall, C. R.; Sazanovich, I. V.; Greetham, G. M.; Bacher, A.; Illarionov, B.; Fischer, M.; Tonge, P. J.; Meech, S. R. Femtosecond to Millisecond Dynamics of Light Induced Allostery in the Avena sativa LOV Domain. *J. Phys. Chem. B* **2017**, *121*, 1010−1019.
(32) Sorigué, D.; Légeret, B.; Cuiné, S.; Blangy, S.; Moulin, S.; Billon, E.; Richaud, P.; Brugière, S.; Couté, Y.; Nurizzo, D.; Müller, P.; Brettel, K.; Pignol, D.; Arnoux, P.; Li-Beisson, Y.; Peltier, G.; Beisson, F. An algal photoenzyme converts fatty acids to hydrocarbons. *Science* **2017**, *357*, 903.
(33) Sandoval, B. A.; Kurtoic, S. I.; Chung, M. M.; Biegasiewicz, K. F.; Hyster, T. K. Photoenzymatic Catalysis Enables Radical-Mediated Ketone Reduction in Ene-Reductases. *Angew. Chem., Int. Ed.* **2019**, *58*, 8714−8718.
(34) Biegasiewicz, K. F.; Cooper, S. J.; Gao, X.; Oblinsky, D. G.; Kim, J. H.; Garfinkle, S. E.; Joyce, L. A.; Sandoval, B. A.; Scholes, G. D.; Hyster, T. K. Photoexcitation of flavoenzymes enables a stereoselective radical cyclization. *Science* **2019**, *364*, 1166.
(35) Wang, X.; Ou, G.; Zhou, K.; Wang, X.; Wang, L.; Zhang, X.; Feng, Y.; Bai, Y.; Wu, H.; Xu, Z.; Ge, J. Targeted Heating of Enzyme Systems Based on Photothermal Materials. *ChemBioChem* **2019**, *20*, 2467−2473.

https://dx.doi.org/10.1021/acs.jpcb.0c04929
J. Phys. Chem. B 2020, 124, 5163−5168